Nanomed Res J 6(4):337-346, Autumn 2021

RESEARCH ARTICLE

Preparation and Characterization of Encapsulated Tamoxifen Citrate-Magnetite Nanoparticle Via Oil in Water Emulsion Evaporation Technique

Emmellie Laura Albert[1], Siti Norzulfikaini Yaacob[2], Ghazaleh Bahmanrokh[1], Toshiki Miyazaki[3], Yuki Shirosaki[4], Che Azurahanim Che Abdullah[1,2,*]

[1] Materials Synthesis and Characterization Laboratory, Institute of Advance Technology, University Putra Malaysia, 43400 UPM Serdang, Selangor, Malaysia

[2] Department of Physics, Faculty of Science, University Putra Malaysia, 43400 UPM Serdang, Selangor, Malaysia

[3] Graduate School of Life Science and Systems Engineering, Kyushu Institute of Technology, 2-4 Hibikino, Wakamatsu-ku, Kitakyushu-shi, Fukuoka, 808-0196; Japan

[4] Graduate School of Engineering, Kyushu Institute of Technology, 1-1 Sensui-cho, Tobata-ku, Kitakyushu-shi, Fukuoka, 804-8550; Japan

ARTICLE INFO

Article History:
Received 07 July 2021
Accepted 16 Oct 2021
Published 01 Nov 2021

Keywords:
Magnetite nanoparticle
Tamoxifen citrate
Poly (d,l-lactice-co-glycolide acid)

ABSTRACT

Current research had successfully encapsulated magnetic nanoparticles (MNP) with selective estrogen receptor drug tamoxifen citrate (TAM) using Poly (d,l-lactice-co-glycolide acid) (PLGA 75:25) via oil in water emulsion technique. TAM is a good example of a drug that is difficult to dissolve. TAM is currently approved for the treatment of hormone-sensitive and early-stage breast cancer as an adjuvant endocrine therapy. The majority of the prescription medicine in today market is made up of poorly soluble, bioavailable, and quickly metabolized and eliminated drug which is a continuously challenges up to these days. Therefore, it is imperative to overcome this disadvantage by encapsulating TAM inside PLGA together with MNP for improved drug delivery. The MNP coated with oleic acid (OA) was synthesized using co-precipitation method and it is known as OAMNP. The fabricated nanohybrid is known as TAM-PLGA-OAMNP where the TAM was encapsulated together with OAMNP within PLGA. XRD results showed that OAMNP is Fe_3O_4. FTIR spectra revealed that the TAM was successfully encased into the PLGA structure. TAM-PLGA-OAMNP average size is about 131 ± 28 nm as shown in TEM results. The nanohybrid nanoparticles showed the absence of hysteresis loop indicative of superparamagnetic properties.

How to cite this article
Laura Albert E., Norzulfikaini Yaacob S., Bahmanrokh Gh., Miyazaki T., Shirosaki Y., Che Abdullah Ch.A. Preparation and Characterization of Encapsulated Tamoxifen Citrate-Magnetite Nanoparticle Via Oil in Water Emulsion Evaporation Technique . Nanomed Res J, 2021; 6(4): 337-346. DOI: 10.22034/nmrj.2021.04.003

INTRODUCTION

Nanoscience is among the most prominent scientific areas of contemporary science. Currently, nanotechnology is being used in the medical, pharmaceutical, robots, computing and tissue engineering sector. It has a numbers of advantages owing to its unique characteristic and small sizes of the nanomaterials [1]. Amongst the unique nanoparticles is magnetic nanoparticles (MNPs) which is a nanoparticles that can be manipulated by the application of external magnetic fields [2]. Nickel (Ni), Iron (Fe), Zinc (Zn), Cobalt (Co) and their chemical compositions are commonly found in magnetic particles. Furthermore, the MNPs' composition is determined by their expected application. The magnetic cores of MNPs are made up of elements including cobalt (Co), nickel (Ni), and neodynium-iron-boron (NIB), which boost magnetic properties however it is easily oxidized and harmful to the human body [3,4].

Nowadays, the most extensively studied MNPs

* Corresponding Author Email: *azurahanim@upm.edu.my*

are ferrite nanoparticles. In general, when the size of the ferrite particle exceeds a critical size, it becomes superparamagnetic, which indicates it can spontaneously become magnetized or demagnetize when external magnetic field exposed or removed to it respectively. As MNPs are incorporated into a living thing, they become magnetized only in the presence of external magnetic fields, which confers on them their special properties and enables their use in biological settings. The MNPs superparamagnetism offer countless advantages, including selective attachment to functional molecules, the ability to provide magnetic properties to the object, and the ability to manipulate and move to a specific position by manipulating the magnetic field generated by an permanent magnet or an electromagnet [5].

MNPs have been used in biomedical applications extensively such as magnetic cell sorting, hyperthermia, MRI contrast agents, and immunoassay pathology laboratories. MNPs were first developed in 2003 for the treatment of hyperthermia and the controlled drug delivery [6]. MNPs and chemotherapeutic drug molecules (doxorubicin) were conjugated using multifunctional magneto-polymeric nanohybrids (MMPN), which are amphiphilic block copolymers. By focusing on the overexpressed HER2/neu cancer marker, the MMPNs is utilised to portray the tumour of breast cancer. In mice implanted with breast cancer xenografts, higher tumor growth suppression is observed when targeted drug delivery are combined in MMNP [7].

Other studies have discovered that drug molecules combined with MNPs were directly triggered in cancer cells. MNPs are used to transport doxorubicin drug to malignant tissue of breast cancer activate them in the tumour setting, resulting in a more targeted and specific breast cancer therapy; the therapeutic impact, in particular, can be monitored using noninvasive MRI. [8]. According to previous studies, MNPs have a promising potential, especially for targeted drug delivery systems. Lipophilic medications were stabilised in circulation thanks to the usage of MNPs as a targeted drug transporter. Furthermore, owing to their superparamagnetic properties, MNPs may be localised at a specific site by utilising an active magnetic field, making MNP a good carrier for selective drug distribution.

Bare MNPs are unsuitable as a drug carrier due to certain constraints, including a limit on the amount of drug transported by the carrier and its drug release speeds. Hence, the MNP is encased with oleic acid (OAMNP) to shield it from degradation and to prevent it from escaping into the body [9,10]. Furthermore, the OA coating minimise the MNP size while also rendering it hydrophobic, allowing it to be integrated in the suggested method of preparing the multifunctional nanocomposite. Furthermore, it may improve the entrapment performance of the MNP within the polymer of preference (PLGA) [11]. The drug is encased in the biodegradable polymer, and the rate of release of the drug can be regulated by the polymer degradation rates [12]. Thus, the MNPs are often coated with silicone as a result of this. Chitosan, gelatin, pullulan, and dextran are examples of natural polymers that can be use for coating MNPs. Additionally, synthetic polymers include poly (ethylene-co-vinyl acetate) (PEVA), PLGA, poly (vinylpyrrolidone) (PVP), poly (ethyleneglycol) (PEG), and poly (vinyl alcohol) (PVA) [13].

Magnetite is commonly encapsulated with PLGA. PLGA was used in nano-emulsion methods to encapsulate MNPs with an anti-cancer medication (Doxorubicin) [14]. Cheng and a colleague encapsulated MNPs with insulin inside PLGA in 2005. Sphere microparticles with average sizes of 4.6 ± 2.2 μm were successfully synthesized [15]. Another studies used PLGA to encapsulated different types of drug such as Methotrexate (MTX) and paclitaxel (PTX) which yield a spherical shape nanoparticles with particle size of 212 nm [16].

Patients with estrogen receptor (ER) positive breast cancer have been treated for more than three decades with tamoxifen citrate (TAM). It inhibits the estrogen receptor from binding to estradiol, thus preventing the receptor from binding to the estrogen-response factor on DNA [17]. Numerous studies have been experimenting with encapsulating MNPs with other drugs. In 2005, PLGA is used to encased MNPs [18], while TAM had been encapsulated using chitosan modified PLGA as in the previous researches [19]. The primary objective of this project is to create a multifunctional nanoparticle with superparamagnetism and therapeutic ability by enclosing MNPs together with TAM in an oil in water emulsion evaporation technique for biomedical purpose.

MATERIALS AND METHODS

Materials

Iron species such as Iron (II) chloride tetrahydrate ($FeCl_2.4H_2O$, 99 %), and iron (III)

chloride hexahydrate ($FeCl_3.6H_2O$, 99 %) were bought from Sigma-Aldrich, Oleic acid ($C_{18}H_{34}O_2$, 99 %), Ammonium hydroxide (NH_4, 32%) purchased from R&M Chemicals. Nitrogen gas (N_2) was supplied from Air Product Malaysia. Polyvinyl alcohol (PVA) (MW: 30 000-70 000), Poly(d,l-lactide-co-glycolide) (PLGA, 75:25) (MW: 66 000-107 000), Tamoxifen citrate (99%), Hydrochloric acid (HCl, 37 %), Dichloromethane (CH_2Cl_2, 90%) obtained from Sigma-Aldrich.

Preparation of Magnetite Nanoparticle and Magnetite Nanoparticles coated with Oleic acid

MNPs were formulated following co-precipitation method with slight modification. Two types of iron salt; $FeCl_2.4H_2O$ and $FeCl_3.6H_2O$ were used as the iron species. Fe^{2+} (ferrous ion) and Fe^{3+} (ferric ion) chloride is dispersed in 150 mL of deionized water in a molar ratio of 1:2 to produce MNPs. Following that, NH_4 (25 mL) was slowly added to the mixture and agitated at 45 °C at an 800 rpm stirring velocity. The precipitation was of a dark brown. A surfactant was added to avoid magnetite from oxidizing and to inhibit aggregation. OA was used as a surfactant. This reaction is about 1 hour. As with the oxidation rate of the iron salt, the particle formation must take place in an environment free of oxygen hence the solution was bubble with N_2 to prevent oxidation. Thus, the particle size would be reduced compare to the one in which no N_2 gas is introduced into the solution [20]. The MNPs encapsulated with OA are called OAMNPs.

Synthesis of Magnetic Polymeric Nanoparticles

The samples were prepared slightly differently than described in previous work [11]. OAMNPs is encapsulated in PLGA using the O/W emulsion technique (75:25). The prepared OAMNPs were then ultrasonically combine with Dichloromethane (DCM) for 5 minutes in an ice bath. Then, PLGA (200 mg) was vortexed until completely dissolve in 2 mL of DCM. Following that, the OAMNPs mixture was mixed with the PLGA solution accompanied by a 3.0 % (w/v) PVA solution via ultrasonication for 5 minutes until the mixture become homogenous. The resulting O/W emulsion solution was diluted by adding 50 mL of a 0.3 % (w/v) aqueous PVA solution. The solution was agitated at 500 rpm for 8 hours to ensure that all organic molecules evaporated completely. PLGA hardened, trapping the OAMNPs within the entangled PLGA. The prepared PLGA-OAMNP was washed with DI water and centrifuge at 9000 rpm for 50 minutes Then the final product was collected and stored in desiccator. The final product is denoted as PLGA-OAMNPs.

Tamoxifen Citrate Loaded into Magnetite Polymeric Nanoparticles

TAM-loaded magnetic polymeric nanoparticles (TAM-PLGA-OAMNP) was prepared using the O/W emulsion evaporation technique. The organic phase was formed by adding around 2 mg of TAM to the PLGA solution and then adding OAMNP. For an additional 5 minutes, the organic phase was sonicated with a 3.0% (w/v) PVA solution. After that, a PVA solution of 0.3 % (w/v) was added to the preceding sample. Since TAM is light sensitive, the evaporation procedure was carried out in the dark. The nanocomposite was washed by centrifugation at 9,000 rpm in order to aid in the removal of impurities and residues. The TAM-PLGA-OAMNPs were prepared through lyophilization for 48 hours, and they were then placed in a desiccator to eliminate moisture. Finally, it was kept in the dark for extended shelf life.

Characterization of MNP, OAMNP, PLGA-OAMNP and PLGA-TAM-OAMNP

The properties of each samples; MNPs, OAMNPs, PLGA-OAMNPs and TAM-PLGA-OAMNPs will be assessed using various instruments such as Fourier transform infrared spectroscopy (FTIR) (Spectrum 100,Perkin Elmer, USA), X-ray diffraction (XRD) (Xpert pro, PANanalytical Philips, The Netherlands), thermalgravimetric analysis (TGA) (TGA/DSC 1 HT, Mettler Toledo, Schweiz), transmission electron microscopy (TEM) (Tecnai TF20 X-Twin, FEI Company, USA), and vibrating sample magnetometer (VSM) (Model 7404, Lake Shore, USA).

XRD is used to analyze atomic spacing and crystal structure of the samples. All powdered samples were placed on quartz plate and exposed to CuKα radiation at wavelength of 1.5406 nm. The samples were measured at room temperatures ranging from 20° to 80°. The data collected were processed using Xpert Software.

The FTIR is used to investigate the functional groups in all the samples. All samples in powder form and placed on the ZnSe crystal. Measurement was taken from 4000-550 cm^{-1} for 4 minutes. The functional band were studies with the aid of IR 2.0

software.

The VSM is used to reveal the magnetization of the prepared MNP targets. The samples were inserted in a thin circular shaped sample holder and then put inside the VSM machine. Measurements conducted at room temperature.

The thermal and physical properties can also be measured using the TGA. All samples are in powder form. The samples were inserted inside the furnace. The furnace was heated at ambient temperature until 800°C with 1K for 1 minute rate, purged with purified N_2 gas. During the measurement, the weight was tracked and recorded.

The shape, surface morphology and size of the samples were investigated using TEM. All samples were dispersed using bath sonicator. The copper mesh was placed inside the solution followed by air drying them. Then, the sample were observed at 200kV of magnification. All images were studies using imageJ software.

RESULTS AND DISCUSSION

X-ray Diffraction Analysis

The crystallinity and purity of the phase of MNPs, OAMNPs, as well as the nanocomposite (TAM-PLGA-OAMNPs and PLGA-OAMNPs) were tested using XRD. Fig. 1 depicts the XRD result of all of the samples in the experiment. The XRD pattern contains diffraction peak at (220), (311), (422), and (440) and (511) indicatives of spinel cubic structure of Fe3O4 (JCPDS: 19-0629). It is apparent that the MNPs and OAMNPs have strong crystalline structure displayed by the intense peaks. XRD data showed that OA and PLGA coating on the MNPs does not have significant effect to the MNPs crystal structure, but the XRD peaks reduced. The XRD peak intensity reduced moderately after OA coating and reduced considerably when it is coated with PLGA. The reason for this is attributed to the OAMNPs being encased by the PLGA. Additionally, the less intense peak is due to the little amount of OAMNP inside PLGA-OAMNPs and TAM-PLGA-OAMNPs supported by the TGA results.

Fourier Transform Infrared Spectroscopy

FTIR studies were carried out on each of them in order to completely comprehend the OA adsorption process on the surface of MNPs. The FTIR spectra of MNPs and OAMNPs is display in Fig. 2. MNPs band at 580 cm^{-1} corresponded to magnetite Fe-O bond, but that it appears at 573 cm^{-1} in OAMNPs which is supported by previous research [21]. Water molecule bands were also found at 1630, 1449, and 3401 cm^{-1}, as documented in the past [22]. In OA, the symmetric and asymmetric CH_2 stretching that was discovered in the previous study relates to two distinct sharp bands at 2918 cm^{-1} and 2849 cm^{-1} [23]. The merger of the carboxyl groups' and OA's double bonds' absorption bands resulted in a strong band at 1710 cm^{-1} in OAMNPs. This indicates that the MNP surface of the OAMNPs has a bilayer cover.

The surface of MNPs is wrapped in OA, as evidenced by the appearance of a band at 1431 cm^{-1} (Vas: COO-) and 1525 cm^{-1} (Vas: COO-) owing to the OA immobilization on the surface of MNPs, in agreement with a previous research [11]. The difference between these two wavenumbers (v) can be used to assess their bonding. Three sorts of interactions may occur between the carboxylates head of OA and the metal atom of MNPs:

- unidentate complex (v = 200-320 cm^{-1}) containing one metal ion bound to one carboxylic

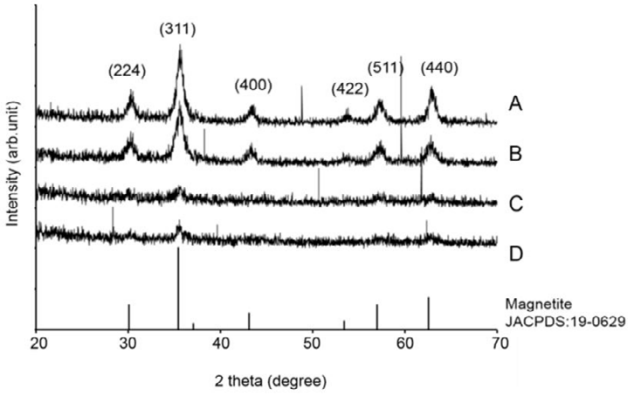

Fig. 1. XRD pattern for (A) MNPs; (B) OAMNPs; (C) PLGA-OAMNPs and (D) TAM-PLGA-OAMNPs

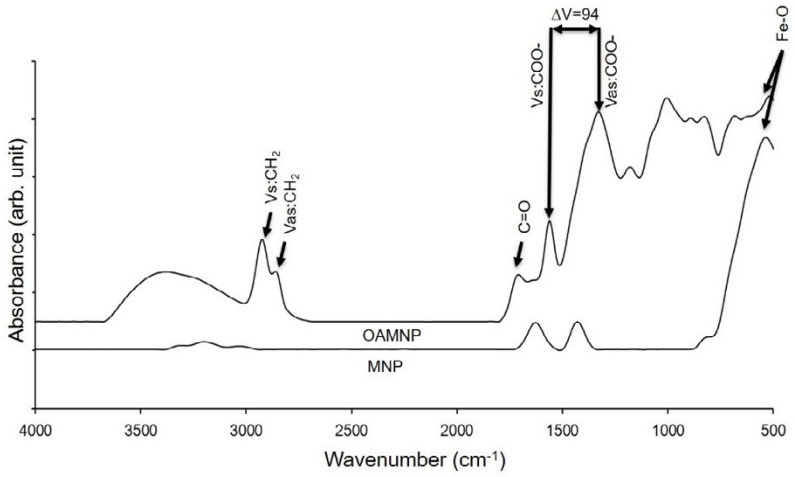

Fig. 2. FTIR spectra of MNP and OAMNP.

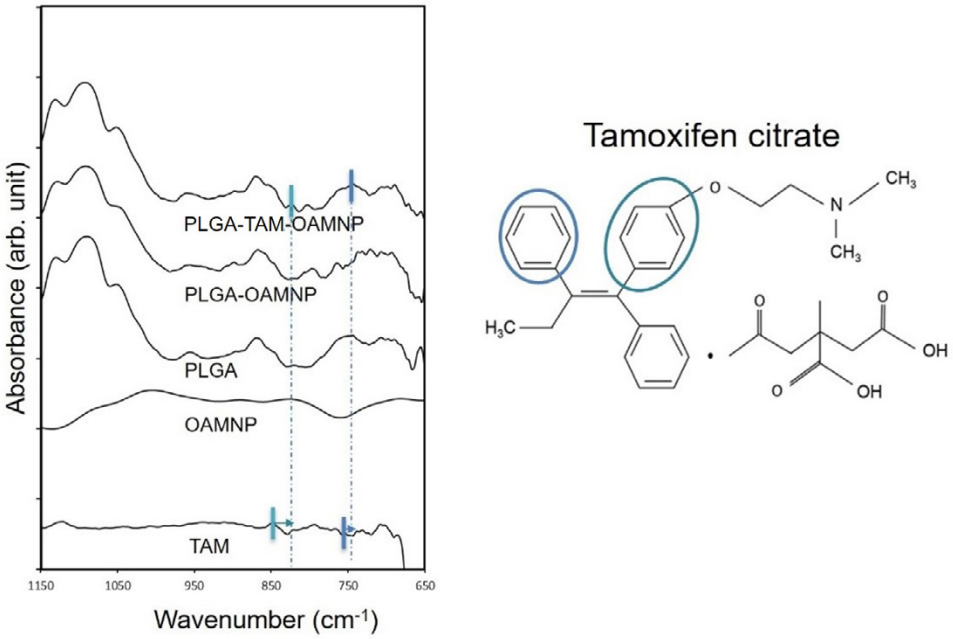

Fig. 3. FTIR spectra of TAM-PLGA-OAMNP, PLGA-OAMNP, PLGA, OAMNP, and TAM at 1150-650cm^{-1} including the chemical structure of Tamoxifen citrate

oxygen atom.

• bidentate complex (chelating) (v < 110 cm^{-1}) one metal ion binds to two carboxylate oxygen molecules.

• bridging complex (v = 140-190 cm^{-1}) consisting of two metal ions bound to two carboxylate oxygen atoms.

It was discovered that the v is 94 in this project, means that they have a bidentate complex. The carboxylate on the surface of MNPs has a covalent bonding pattern hence it was established that the surface of MNP has chemisorbed OA.

Additionally, the FTIR is used to determine the bond interaction between the TAM, OAMNPs, and PLGA as shown in Fig. 4. The PLGA bands significantly dominate the FTIR spectra of the TAM-PLGA-OAMNPs and PLGA-OAMNPs. The TAM and OAMNPs FTIR bands were masked by the strong PLGA bands, which is corroborated by the TGA data, indicating that the nanoparticles are mostly composed of PLGA. The prominent bands at 1754 cm^{-1} in the TAM-PLGA-OAMNPs are

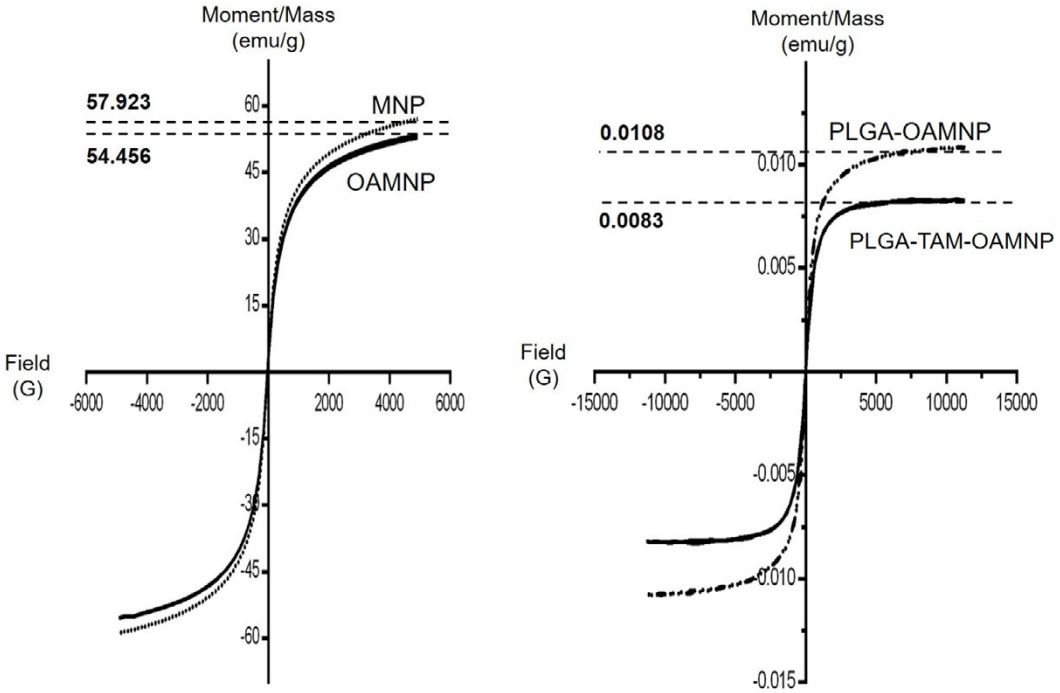

Fig. 4. VSM curve for (A) MNPs, (B) OAMNPs, (C) PLGA-OAMNPs, and (D) TAM-PLGA-OAMNPs

Table 1. The temperature attribute to the percentage weight loss of the MNP, OAMNP, TAM-PLGA-OAMNP, and PLGA-OAMNP

Samples	Temperature (°C)	Percentage weight loss (%)
MNP	25-102	7.8
	103-282	4.5
	283-800	3.5
OAMNP	25-139	3.9
	140-269	7.1
	270-323	2.3
	333-423	5.0
	424-800	9.7
PLGA-OAMNP	25-279	7.6
	280-308	57.0
	309-800	2.4
TAM-PLGA- OAMNP	25-262	4.0
	263-303	60.5
	303-800	9.5

caused by the ketonic group, belonging to PLGA and OA.

Small bands found in TAM-PLGA-OAMNPs at 825 cm^{-1} and 756 cm^{-1} pertain to TAM's 1, 4-benzene substitution and mono-substitute benzene, correspondingly. Another small bands of 825 cm^{-1} and 756 cm^{-1} observed in TAM-PLGA-OAMNPs correlate, accordingly, to 1, 4-benzene and mono-benzene substitution belonging to TAM. Fig. 3 demonstrates that the chemical structure of TAM includes both benzene replacements, suggesting that the PLGA encapsulated TAM. Moreover, the bands of over 3000 cm^{-1}, which are found in both PLGA and OA, might attribute to the CH^2 stretch which indicates, OA presence in OAMNP inside the PLGA matrix.

Magnetic Properties

The magnetic characteristics of MNPs, OAMNPs, TAM-PLGA-OAMNPs, and PLGA-

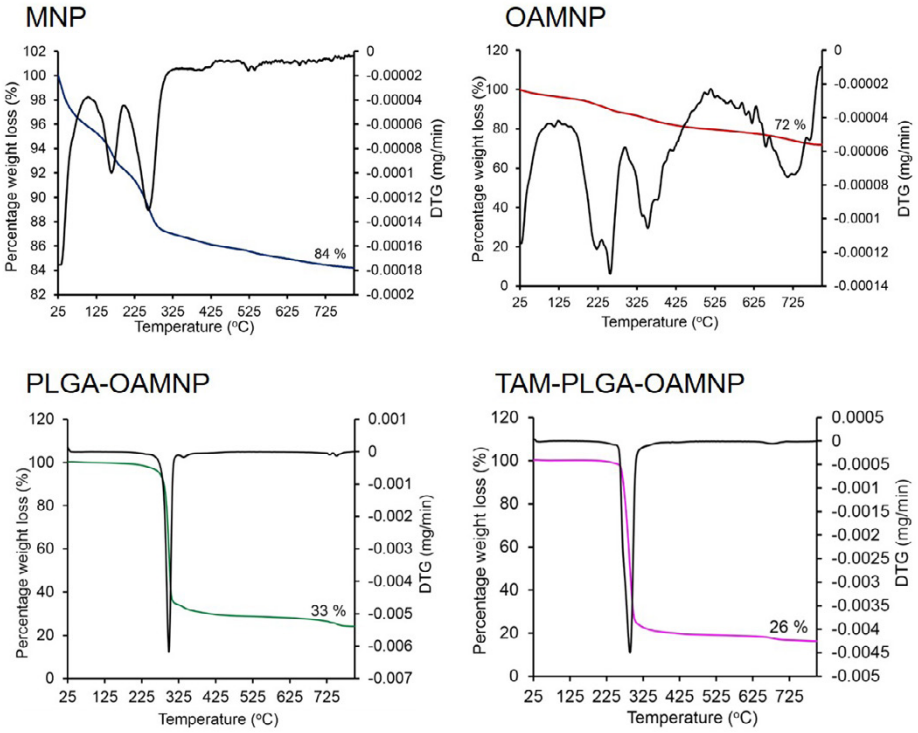

Fig. 5. TGA/ DTG curve of A) MNP, B) OAMNP, C) PLGA-OAMNP and D) PLGA-TAM-OAMNP at 25°C to 800°C.

OAMNPs were investigated using VSM. About 57.923 emu/g and 54.356 emu/g magnetic saturation (Ms) were reported for MNPs and OAMNPs, accordingly. The Ms value was slightly reduced owing to the non-magnetic feature of the OA layer on the MNP surface consistent with previous work [24]. The electron transfer between its Fe atoms in OAMNPs shifted the surface spin and magnetic anisotropy of the Fe atom. The observed findings, as shown in Fig. 6, were consistent with those previously published [25]. All of the samples had superparamagnetic curves based on the VSM findings. Additionally, they do not exhibit coercivity and remanence. The absence of a hysteresis loop in all samples confirms the materials' superparamagnetic properties, which makes them ideal for biological applications.

For PLGA-OAMNPs, the Ms value is 10.812 x 10^{-3} emu/g. In contrast, for TAM-PLGA-OAMNPs, the Ms value is 8.3096 x 10^{-3} emu/g as seen in Fig. 4. Once nanoparticles are enclosed in PLGA, the Ms value is decreased substantially. Following encapsulation in PLGA, the Ms value was reduced significantly due to the presence of non-magnetic materials and the exchange of electrons between Fe atoms in OAMNPs, as described in the past research [26]. As expected, these particles exhibited superparamagnetic behaviour, which is required for medical application, such as magnetic resonance imaging (MRI) and is demonstrated by the absence of a hysteresis loop and negligible coercivity. These particles also indicated that they behaved as a single-domain MNPs in as supported by previous research [27].

Thermogravimetric Analysis

TGA was used to determine the weight loss of all samples as the temperature increases gradually to 800 °C in the presence of Nitrogen gas as shown in Fig. 5. MNPs lose about 12.3 % of their weight at temperatures below 282 °C owing to the loss of water at the nanoparticle's surface and water bound inside the MNPs in relation to the DTG peaks at 163 °C and 260 °C. Likewise, OAMNPs lose roughly 11% of their weight at temperatures ranging from 25 until 269 °C. The two metal sites (Fe) interacting with the carboxylate cause two weight losses for OA in OAMNPs at 270 to 323 °C and 324 to 423 °C. DTG peak at 262 °C and 323 °C corresponded to a weight loss of 7.3 % consistent with earlier studied [28]. At

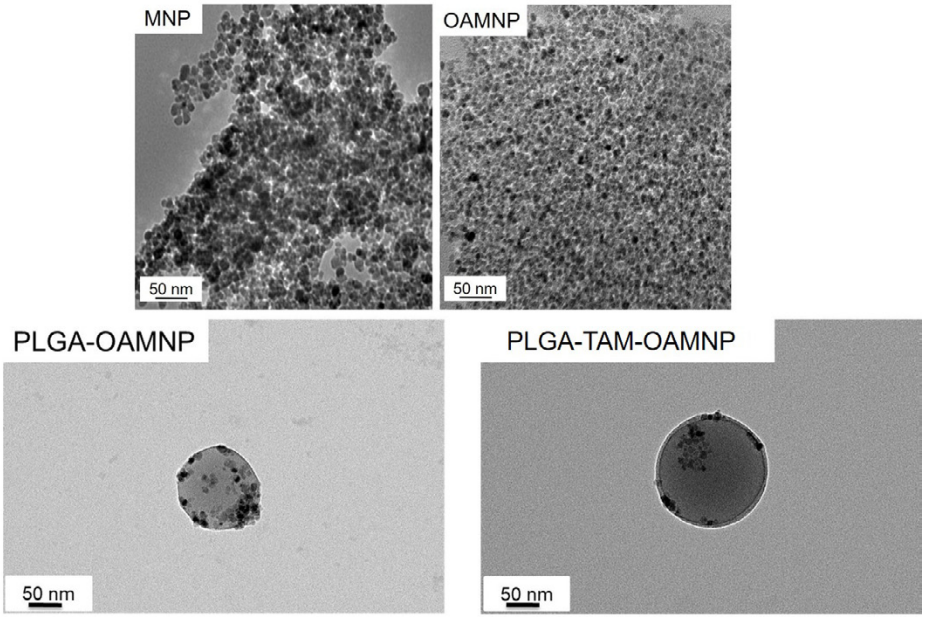

Fig. 6. TEM images of MNP, OAMNP, PLGA-TAM-OAMNP, and PLGA-OAMNP.

temperatures ranging from 423 to 800 °C, a weight loss of around 2.6 % was reported. This is due to Fe_3O_4 being reduced to FeO which corresponds to the DTG maxima at 701 °C.

OAMNPs lose around 28 %, while MNPs lose around 16 %. OAMNPs lose more weight than MNPs because of the OA coating. The initial weight loss occurred between 25 and 279 °C, and around 7.6 % of the PLGA-OAMNPs weight was lost. TAM-PLGA-OAMNPs weight reduce by around 4 % between 25 and 262 °C attributed to moisture loss. Another weight loss occurred between 263 and 303 °C, and about 60.5 % in agreement with the DTG maxima at 285 °C.

The increase in temperature causes the degradation of PLGA as anticipated. The PLGA-OAMNP lose about 57.0% because it exhibits same thermal trend between 280 and 303 °C at 294 °C of DTG peak. Previous studies indicated a one-step degradation of PLGA (75:25) which is similar to the current project [29]. The degradation of PLGA mainly due to the non-radical backbiting ester interchange which include the OH chain end, which is mostly linear cyclic oligomers and monomers, acetaldehyde belong to polylactic acid, methyl glycolate from polyglycolic acid, PLGA are consist of carbon dioxide, polylactic acid and polyglycolic acid so the second output are from the decarboxylation of terminal carboxyl.

PLGA decompose to carbon monoxide, methylketene, ketene, and formaldehyde through the radical chain scission process when the temperature rises. The breakdown output of PLGA are comparable to polylactic acid and polyglycolic acid polymers [30]. Additionally, TAM-PLGA-OAMNPs begin weight loss at 263 °C earlier compared to PLGA-OAMNPs degraded at 280 °C.

At 147 °C TAM deteriorates, whereas at 236 °C PLGA degrades. TAM-PLGA-OAMNPs have nearly comparable thermal behavior to PLGA-OAMNPs, but its degradation begins earlier, indicating the presence of encapsulated medication on the nanosphere and due to TAM low melting point of around 256 °C.

After the degradation of TAM, PLGA, and OA, only MNP remains. The presence of TAM inside TAM-PLGA-OAMNP is linked to the fact that TAM-PLGA-OAMNP loses more weight than PLGA-OAMNP. The obtained TGA curve is comparable to those previously reported [27,31]. After the breakdown of PLGA, TAM, and OA in the composite particles, finally MNP decompose further; hence, the percentage of MNPs can be estimated, which is approximately 33 % for TAM-PLGA-OAMNPs and 26 % for PLGA-OAMNPs.

Transmission Electron Microscopy

TEM was employed to characterize the shape and size features of MNPs, OAMNPs, TAM-PLGA-OAMNPs, and PLGA-OAMNPs as in Fig. 6. MNPs

were found to be polydisperse and aggregated owing to their high surface to volume ratio, in order to minimize their surface energy. steric repulsion is often used to avoid aggregation as supported by previous research [9].

OAMNPs were scattered to some extent owing to the OA coating, as evidenced by the TEM picture. MNPs and OAMNPs have a spherical structure with a diameter of around 10±2 nm and 8±1 nm, respectively. Due to the thin covering of the OA, the size decreased which is in alignment with previous finding [32].

The OAMNP aggregates within the PLGA matrix in TAM-PLGA-OAMNPs and PLGA-OAMNPS. OAMNPs were successfully encased within PLGA. OAMNPs also have an inclination toward the surface of the PLGA matrix, which might be due to surface tension. Chen et al. (2020) and Zumaya et al. (2020) have recently published work with a similar morphology, in which the MNPs are encased within spherical PLGA nanoparticles [33,34]. TAM-PLGA-OAMNPs and PLGA-OAMNPs were found to have sizes of about 131±28 nm and 80±28 nm, respectively. TAM encapsulation resulted in TAM-PLGA-OAMNPs increasing size is in agreement with previous work which indicated the increase in size when the drug is added [35]. As a result, the TAM-PLGA-OAMNP sizes are suitable for targeted medication delivery to cancer locations because the majority of cutoff diameter of porous blood arteries in majority of tumors are 380-780 nm as stated in previous work [36].

CONCLUSION

MNPs and OAMNPs were produced successfully using the co-precipitation technique. MNPs and OAMNPs have an exceptionally small size, less than 11 nm, and therefore possess superparamagnetic characteristics. The OA coating was effective in reducing MNP agglomeration. OAMNPs and TAM were successfully encapsulated in PLGA (75:15). They were encapsulated using an O/W emulsion and evaporation method. The Ms of the TAM-PLGA-OAMNPs decreased following encapsulation with PLGA, but their superparamagnetic characteristics remained. Additionally, the size of TAM-PLGA-OAMNPs was determined to be about 132 nm using a TEM which is smaller in comparison to the findings by previous researchers, indicated the appropriateness for biological applications [33-34].

ACKNOWLEDGEMENTS

The author wishes to express her gratitude to the late Dr Mansor Hashim for the support and supervision in term of magnetic materials. The part of this work was supported by the programs in “Promotion and Standardization of the Tenure-Track System (Kojinsenbatsu)” financed by Ministry of Education Culture, Sports, Science and Technology (MEXT), Student Exchange Support Program financed by Japan Student Services Organization and Putra Group Initiative (IPB) Research Grant financed by Universiti Putra Malaysia.

CONFLICTS OF INTEREST

The authors declare that there are no conflicts of interest.

REFERENCES

1. Khan I, Saeed K, Khan I. Nanoparticles: Properties, applications and toxicities. Arab J Chem [Internet]. 2019;12(7):908–31. Available from: http://dx.doi.org/10.1016/j.arabjc.2017.05.011
2. Biehl P, von der Lühe M, Dutz S, Schacher FH. Synthesis, characterization, and applications of magnetic nanoparticles featuring polyzwitterionic coatings. Polymers (Basel). 2018;10(1).
3. Woo K, Hong J, Choi S, Lee H-W, Ahn J-P, Kim CS, et al. Easy synthesis and magnetic properties of iron oxide nanoparticles. Chem Mater. 2004;16(14):2814–8.
4. Faraji M, Yamini Y, Rezaee M. Synthesis , Stabilization , Functionalization , Characterization , and Applications. J Iran Chem Soc. 2010;7(1):1–37.
5. Kodama RH. Magnetic nanoparticles. J Magn Magn Mater. 1999;200:359–72.
6. Pankhurst QA, Connolly J, Jones SK, Dobson J. Applications of magnetic nanoparticles in biomedicine. J Phys D Appl Phys [Internet]. 2003;36:R167. Available from: http://stacks.iop.org/0022-3727/36/i=13/a=201
7. Yang J, Lee C-H, Ko H-J, Suh J-S, Yoon H-G, Lee K, et al. Multifunctional Magneto-Polymeric Nanohybrids for Targeted Detection and Synergistic Therapeutic Effects on Breast Cancer. Angew Chemie [Internet]. 2007;119:8992–5. Available from: http://onlinelibrary.wiley.com/store/10.1002/ange.200703554/asset/8992_ftp.f?v=1&t=j4w0vj13 &s=81c-63cd75d0cde12e9cc1653245569be5b18e505
8. Yigit M V, Moore A, Medarova Z. Magnetic Nanoparticles for Cancer Diagnosis and Therapy. Pharm Res [Internet]. 2012 Jul 9;29:1180–8. Available from: https://link.springer.com/content/pdf/10.1007%2Fs11095-012-0679-7.pdf
9. Andhariya N, Chudasama B, Mehta R V, Upadhyay R V. Biodegradable thermoresponsive polymeric magnetic nanoparticles: a new drug delivery platform for doxorubicin. J Nanoparticle Res [Internet]. 2011 Jul 7;13:1677–88. Available from: https://link.springer.com/content/pdf/10.1007%2Fs11051-010-9921-6.pdf
10. McBain SC, Yiu HHP, Dobson J. Magnetic nanoparticles for gene and drug delivery. Int J Nanomedicine [Internet]. 2008;3:169–80. Available from: https://www.ncbi.nlm.nih.

gov/pmc/articles/PMC2527670/pdf/ijn-0302-169.pdf
11. Okassa LN, Marchais H, Douziech-Eyrolles L, Cohen-Jonathan S, Soucé M, Dubois P, et al. Development and characterization of sub-micron poly(d,l-lactide-co-glycolide) particles loaded with magnetite/maghemite nanoparticles. Int J Pharm. 2005;302(1):187–96.
12. Arias JL, Gallardo V, Gómez-Lopera SA, Plaza RC, Delgado A V. Synthesis and characterization of poly(ethyl-2-cyanoacrylate) nanoparticles with a magnetic core. J Control Release [Internet]. 2001;77:309–21. Available from: http://www.sciencedirect.com/science/article/pii/S0168365901005193
13. Yang J, Park S-B, Yoon H-G, Huh Y-M, Haam S. Preparation of poly ε-caprolactone nanoparticles containing magnetite for magnetic drug carrier. Int J Pharm. 2006;324(2):185–90.
14. Gupta AK, Gupta M. Synthesis and surface engineering of iron oxide nanoparticles for biomedical applications. Biomaterials. 2005;26:3995–4021.
15. Cheng J, Yim CH, Teply B a, Ho D, Farokhzad OC, Langer RS. Magnetite-PLGA microparticles for oral delivery of insulin. 2005;873E(Biological and Bio-Inspired Materials and Devices):No pp. given, Paper #: K5.8.
16. Madani F, Esnaashari SS, Bergonzi MC, Webster TJ, Younes HM, Khosravani M, et al. Paclitaxel/methotrexate co-loaded PLGA nanoparticles in glioblastoma treatment: Formulation development and in vitro antitumor activity evaluation. Life Sci [Internet]. 2020;256(June):117943. Available from: https://doi.org/10.1016/j.lfs.2020.117943
17. Hu R, Hilakivi-Clarke L, Clarke R. Molecular mechanisms of tamoxifen-associated endometrial cancer (Review). Oncol Lett [Internet]. 2015 Aug 2;9:1495–501. Available from: http://www.spandidos-publications.com/ol/9/4/1495/download
18. Lee S-J, Jeong J-R, Shin S-C, Kim J-C, Chang Y-H, Lee K-H, et al. Magnetic enhancement of iron oxide nanoparticles encapsulated with poly (D, L-latide-co-glycolide). Colloids Surfaces A Physicochem Eng Asp. 2005;255(1–3):19–25.
19. Thakur CK, Thotakura N, Kumar R, Kumar P, Singh B, Chitkara D, et al. Chitosan-modified PLGA polymeric nanocarriers with better delivery potential for tamoxifen. Int J Biol Macromol. 2016;93:381–9.
20. Ali A, Zafar H, Zia M, Ul Haq I, Phull AR, Ali JS, et al. Synthesis, characterization, applications, and challenges of iron oxide nanoparticles. Nanotechnol Sci Appl [Internet]. 2016 [cited 2017 Sep 17];9:49–67. Available from: http://www.ncbi.nlm.nih.gov/pubmed/27578966
21. Kandpal ND, Sah N, Loshali R, Joshi R, Prasad J. Co-precipitation method of synthesis and characterization of iron oxide nanoparticles. J Sci Ind Res [Internet]. 2014;73(2):87–90. Available from: http://nopr.niscair.res.in/bitstream/123456789/26444/1/JSIR 73%282%29 87-90.pdf
22. Zhang L, He R, Gu H-C. Oleic acid coating on the monodisperse magnetite nanoparticles. Appl Surf Sci [Internet]. 2006 Dec [cited 2015 Nov 9];253(5):2611–7. Available from: http://www.sciencedirect.com/science/article/pii/S0169433206007197
23. Coates J, Ed RAM. Interpretation of Infrared Spectra , A Practical Approach Interpretation of Infrared Spectra. Interpret a J Bible Theol. 2000;10815–37.
24. Cui YN, Xu QX, Davoodi P, Wang DP, Wang CH. Enhanced intracellular delivery and controlled drug release of magnetic PLGA nanoparticles modified with transferrin. Acta Pharmacol Sin [Internet]. 2017;38(6):943–53. Available from: http://dx.doi.org/10.1038/aps.2017.45
25. Liu X, Kaminski MD, Guan Y, Chen H, Liu H, Rosengart AJ. Preparation and characterization of hydrophobic superparamagnetic magnetite gel. J Magn Magn Mater [Internet]. 2006;306:248–53. Available from: http://www.sciencedirect.com/science/article/pii/S0304885306006354
26. Dorniani D, Kura AU, Hussein-Al-Ali SH, Bin Hussein MZ, Fakurazi S, Shaari AH, et al. In vitro sustained release study of gallic acid coated with magnetite-PEG and magnetite-PVA for drug delivery system. Sci World J [Internet]. 2014 [cited 2017 Apr 11];2014:416354. Available from: http://www.ncbi.nlm.nih.gov/pubmed/24737969
27. Bootdee K, Nithitanakul M, Grady BP. Synthesis and encapsulation of magnetite nanoparticles in PLGA: effect of amount of PLGA on characteristics of encapsulated nanoparticles. Polym Bull [Internet]. 2012 Oct 21 [cited 2017 Jan 9];69(7):795–806. Available from: http://link.springer.com/10.1007/s00289-012-0773-3
28. Astete CE, Kumar CSSR, Sabliov CM. Size control of poly(d,l-lactide-co-glycolide) and poly(d,l-lactide-co-glycolide)-magnetite nanoparticles synthesized by emulsion evaporation technique. Colloids Surfaces A Physicochem Eng Asp [Internet]. 2007 May [cited 2016 Feb 16];299(1–3):209–16. Available from: http://www.sciencedirect.com/science/article/pii/S0927775706008892
29. Yang Z, Peng H, Wang W, Liu T. Crystallization behavior of poly(ε-caprolactone)/layered double hydroxide nanocomposites. J Appl Polym Sci. 2010;116(5):2658–67.
30. Palacios J, Albano C, González G, Castillo RV, Karam A, Covis M. Characterization and thermal degradation of poly(d,l-lactide-co-glycolide) composites with nanofillers. Polym Eng Sci [Internet]. 2013;53:1414–29. Available from: http://onlinelibrary.wiley.com/doi/10.1002/pen.23396/abstract
31. Pérez A, Mijangos C, Hernández R. Preparation of Hybrid Fe_3O_4 /Poly(lactic- co -glycolic acid) (PLGA) Particles by Emulsion and Evaporation Method. Optimization of the Experimental Parameters. Macromol Symp [Internet]. 2014 Jan [cited 2017 Mar 4];335(1):62–9. Available from: http://doi.wiley.com/10.1002/masy.201200123
32. Mahdavi M, Namvar F, Ahmad M Bin, Mohamad R. Green biosynthesis and characterization of magnetic iron oxide (Fe 3O4) nanoparticles using seaweed (Sargassum muticum) aqueous extract. Molecules. 2013;
33. Chen HA, Ma YH, Hsu TY, Chen JP. Preparation of peptide and recombinant tissue plasminogen activator conjugated poly(Lactic-co-glycolic acid) (PLGA) magnetic nanoparticles for dual targeted thrombolytic therapy. Int J Mol Sci. 2020;21(8).
34. Zumaya ALV, Martynek D, Bautkinová T, Šoóš M, Ulbrich P, Raquez JM, et al. Self-assembly of poly(L-lactide-co-glycolide) and magnetic nanoparticles into nanoclusters for controlled drug delivery. Eur Polym J [Internet]. 2020;133(May):109795. Available from: https://doi.org/10.1016/j.eurpolymj.2020.109795
35. Madani F, Esnaashari SS, Mujokoro B, Dorkoosh F, Khosravani M, Adabi M. Investigation of effective parameters on size of paclitaxel loaded PLGA nanoparticles. Adv Pharm Bull [Internet]. 2018;8(1):77–84. Available from: https://doi.org/10.15171/apb.2018.010
36. Bae YH, Park K. Targeted drug delivery to tumors: Myths, reality and possibility. Vol. 153, Journal of Controlled Release. 2011. p. 198–205.